The Transient Modeling of Bubble Pinch-Off Using an ALE Moving Mesh

Christopher J. Forster, Marc K. Smith*
School of Mechanical Engineering, Georgia Institute of Technology
*Corresponding author: 771 Ferst Drive NW, Atlanta, GA 30332-0405, marc.smith@me.gatech.edu

Abstract: The use of an acoustic field to control the boiling process has the potential to increase the overall rate of heat transfer and delay the critical transition to film boiling. This system is being investigated through the development of a model of a single boiling bubble near a flat, heated, horizontal surface in the presence of an acoustic field. The dynamics of the bubble interface is modeled using the Arbitrary Lagrangian-Eulerian (ALE) Moving Mesh method, which offers a sharp interface to apply conditions for surface tension and the modeling of other physics, such as acoustic fields and evaporation. However, the disadvantage of the ALE method is its difficulty in dealing with changes in topology, such as bubble pinch-off. In this paper, pinch-off is investigated using a simpler model of the transient motion of a single, isothermal bubble attached to the bottom surface of a water tank that rises under the effect of buoyancy, detaches from the surface, and then continues to rise. The change in topology, pinch-off, is handled in a Matlab script before returning to Comsol to complete the simulation. The resulting simulation is compared in terms of accuracy and computational expense to similar simulations based on the level-set and phase-field application modes.

Keywords: ALE, moving mesh, pinch-off, surface tension, dynamic contact line

1. Introduction

In modeling of boiling heat transfer near a flat, heated, horizontal surface, the details of the bubbles' liquid-gas interface evolution in time are important in the determination of the critical transition to film boiling. Previous work in this area includes the use of level-set and phase-field models [1,2]. These have the advantage of handling changes in topology within the models themselves. However, while level-set and phase-field models handle these changes in topology, they lack accuracy, for example, in the necking region of a bubble. When the necking region reduces to approximately the same length scale as the mesh elements, the phase tracking (or level sets) can no longer resolve these areas accurately. The neck may then pinch-off in a way that does not accurately reflect the appropriate physics.

Level-set and phase-field models offer a diffuse boundary that is not ideal for modeling heat transfer or pressure acoustic interactions near fluid interfaces. The ALE moving mesh directly tracks the free surfaces and allows for a sharp interface to apply boundary conditions. The number of elements and computational expense is another factor in selecting the type of model to use. The ALE method generally requires less memory and processing time, but it does require more time from the user to setup the model and periodically remesh. This can be automated by using a script in many cases. If there are events that occur at selective times during the transient simulation, the mesh may need refinement local to the time of the event to resolve flow structures that may temporarily arise. This is true with bubbles going through large deformations after pinch-off. The oscillations eventually damp out and as the bubble rises through the surrounding fluid a more coarse mesh may be used as the oscillations lessen.

In this paper, these three numerical methods are compared in how they handle pinch-off using a model of a single isothermal gas bubble being pulled away from a horizontal surface by buoyancy. The model is 2D axisymmetric with separate fluid domains for the bubble and the surrounding liquid. The fluids are treated as incompressible and Newtonian. The bubble contact line is dynamic and the contact angle is fixed at 50°, defined as the angle interior to the bubble. While the contact angle is set at 50° in this model, it can be changed or defined as a function of another variable, such as temperature. The ALE model is compared to the conservative level-set and phase-field models with identical initial geometries and fluid

properties. The Bond and Morton numbers can be used together to characterize bubble shapes and terminal velocities [3]. Individually, the Bond number represents the ratio of gravitational to surface tension forces, and the Morton number is a dimensionless combination of viscous, capillary, and viscous forces. The Bond number is 4.395 based on a length scale of the radius of a sphere with equal volume as the bubble. The Morton number is 9.597e-8.

2. Use of COMSOL Multiphysics

2.1 Initial Model Geometry and Boundary Conditions

The bubble begins in a deformed configuration wetted to the bottom surface of a tank. Axial symmetry is used to simplify the model and reduce the size of the domain to be modeled. The boundaries and sub-domains are shown in Figure 1 below.

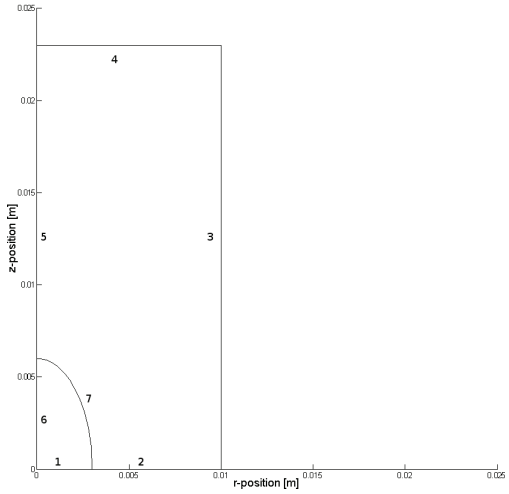

Figure 1. Initial geometry before pinch-off. Each boundary is labeled to identify the boundary conditions listed in Table 1.

The moving mesh boundary conditions applied at the tank walls, open top, and axial symmetry line enforce zero normal displacement. The moving mesh boundary conditions for the free surface force the mesh velocity to match the interface normal velocity. Tangential motion of the mesh is allowed at all boundaries. The tangential mesh movement allows for higher mesh quality with larger mesh deformations.

Table 1. Fluid Domain Boundary Conditions for the ALE Model.

Boundary Number	Type	Condition Satisfied
1	Wall	No Penetration, Slip
2	Wall	No Penetration, Slip
3	Wall	No Penetration, Slip
4	Open Boundary	Zero Gage Pressure
5	Symmetry	Axial Symmetry
6	Symmetry	Axial Symmetry
7 (inside)	General Stress	Pressure, Continuity of Shear Stress
7 (outside)	Moving Wall	No Slip at Fluid Interface

The boundary conditions on the inner surface of the free interface are a stress condition that implements continuity of shear stress at the interface, but indirectly enforces a no-flux condition. This is handled by the moving mesh velocity being specified as the normal velocity of the fluid inside the bubble immediately at the interface. A tangential velocity of the mesh is allowed on the free surface, but the normal velocity matching between the fluid at the inner surface of the bubble interface and the mesh velocity prevents a mass flux across the free surface. The outer surface of the interface behaves as a moving wall to displace the surrounding fluid as the bubble moves; the moving wall velocity is matched to the velocity of the fluid inside the bubble at the free surface.

The surface tension is implemented at the free surface directly using weak boundary expressions. The contact angle of the dynamic contact line, at the intersection of boundaries 1, 2, and 7, is enforced using weak point expressions.

2.2 Pinch-Off Transition

Leading up to pinch-off the ALE model is run with remeshing periodically to maintain mesh quality. The pinch-off point is chosen near the minimum neck radius for this simulation. A reasonable gap height is chosen between the attached and pinched bubble to prevent creating excessively small elements in the pinched region.

The final geometry of the attached bubble simulation is exported to Matlab as an array of points with the pinch-off points inserted. The boundary points are spline-fit with constraints on end-point tangency. The geometry is imported back into Comsol and boundary conditions are transferred from the previous geometry. The number of fluid domains, and Navier-Stokes equation sets, increase from two to three domains. Since a finite amount of time occurs during pinch-off, which is not modeled here, post-pinch-off velocity and pressure fields were estimated to continue the simulation. These estimated initial conditions after pinch-off demonstrate that it is possible to continue the new model where the previous model ended. Figure 2 compares the final geometry of the attached bubble and the bubbles immediately after pinch-off. Figures 3-4 show the initial conditions after pinch-off.

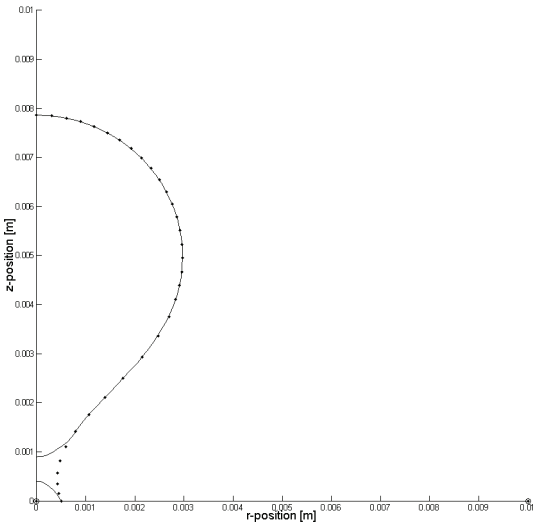

Figure 2. New geometry after pinch-off with previous geometry points overlaid.

The pressure distribution in Figure 3 approximates the appropriate initial conditions after pinch-off by accounting for hydrostatic pressure with an upper boundary at zero gage pressure and Young-Laplace pressure jumps at the fluid interfaces. The attached bubble has smaller radii of curvature, so its internal pressure is greater than that of the detached bubble. In addition to the hydrostatic pressure component, a dynamic pressure drop occurs in areas of higher velocity magnitude. This can be seen in Figure 3 by the typical hydrostatic pressure variation near the top and side of the tank, and the lower-pressure region in the vicinity of the pinch-off point. The pressure drops due to the radially inward and axially upward velocity in the bubble's wake.

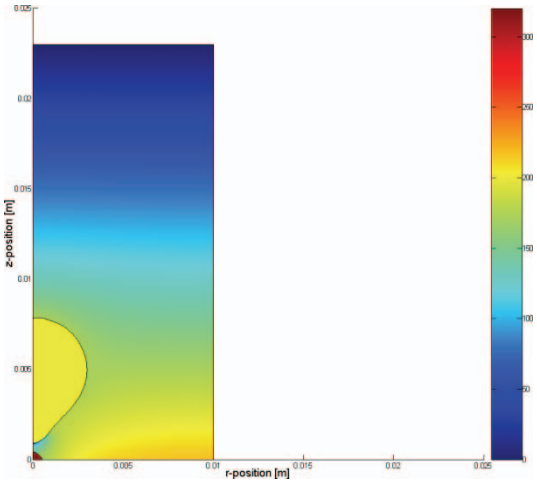

Figure 3. The initial post-pinch-off pressure distribution mapped over the new domains.

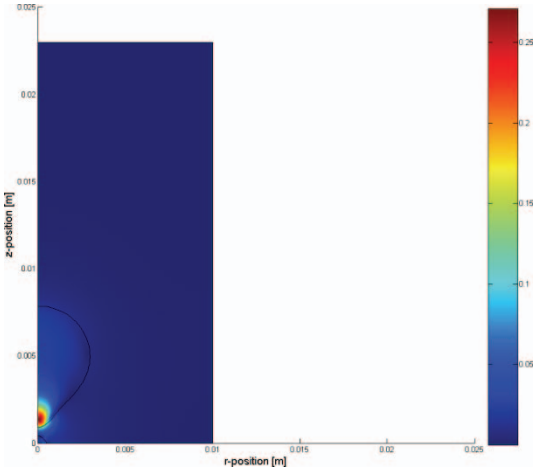

Figure 4. The initial post-pinch-off velocity magnitude distribution mapped over the new domains.

The velocity field shown in Figure 4 is a result of the surrounding fluid having a larger dynamic viscosity and a density three orders of magnitude larger than that of the bubble. The fluid moving inside of the bubble pinching region reaches a relatively high velocity as the flow area at the neck is being reduced. However, this is reduced

some as the surrounding fluid, moving at a lower speed, fills the gap volume due to the relatively large inertia of this slower-moving fluid. The fluid velocities are also matched at the fluid interface. The mapped initial conditions also satisfy symmetry conditions required to find consistent initial conditions in the axisymmetric geometry.

The pinch-off criteria will be improved in future work. When the bubble neck is small enough, the pinch-off process will be computed analytically using a separate asymptotic model. This will reduce numerical computational requirements due to meshing regions of relatively small length scales compared to the rest of the model. After pinch-off, the shape of the gas bubbles and the associated velocity and pressure fields near the pinch-off point will be used to reinitialize the numerical model and continue the simulation. This asymptotic model will also conserve the volume of both fluids, which is clearly not done in the present work.

2.3 Governing Equations

The normal-stress boundary condition on the liquid-gas interface is

$$\left(\underline{\sigma}_l - \underline{\sigma}_g\right)\hat{n} = \sigma\kappa\hat{n},$$

where $\underline{\sigma}_{g,l}$ are the stress tensors for the gas and the liquid, defined as

$$\underline{\sigma}_{g,l} = \left[-P\underline{I} + \eta\left(\nabla\underline{u} + \left(\nabla\underline{u}\right)^T\right)\right]_{g,l}$$

$\hat{n}$ is the outward unit normal to the gas-liquid interface, σ is the surface tension of the interface, and κ is the curvature of the interface defined as

$$\kappa = \nabla_s \cdot \hat{n},$$

where ∇_s is the surface divergence operator. The Navier-Stokes equations on the sub-domains remain unchanged since the surface tension is implemented as a boundary condition.

Multiplying both sides of the first equation by a test function and integrating results in,

$$\int_{\partial\Omega}\left(\tilde{\varphi}\underline{\sigma}_l\hat{n}\right)dA = \int_{\partial\Omega}\left(\tilde{\varphi}\underline{\sigma}_g\hat{n}\right)dA + \int_{\partial\Omega}\left(\tilde{\varphi}\sigma\kappa\hat{n}\right)dA.$$

Applying the surface divergence theorem [4] to the last surface integral on the right-hand side and substituting back in yields,

$$\int_{\partial\Omega}\left(\tilde{\varphi}\underline{\sigma}_l\hat{n}\right)dA = \int_{\partial\Omega}\left(\tilde{\varphi}\underline{\sigma}_g\hat{n}\right)dA - \int_{\partial\Omega}\left(\sigma\nabla_s\tilde{\varphi}\right)dA + \int_{\partial^2\Omega}\left(\sigma\tilde{\varphi}\hat{m}\right)ds,$$

where $\hat{m}$ is a unit binormal vector at the contact line, and $\tilde{\varphi}$ is a test function.

This last equation can be applied as boundary and point weak expressions in Comsol. This applies to 2D, 2D axisymmetric, and 3D models, although some minor modifications need to be made to express this in polar coordinates.

3. Results and Discussion

3.1 ALE Results

The ALE moving mesh simulation required 13 meshes to move from an attached bubble, transition through pinch-off, and rise to the top of the tank, due to buoyancy of the bubble in the surrounding fluid. Figure 5 illustrates some, but not all, of the geometries after remeshing throughout the simulation. The approximate calculation time on a 2.2 GHz dual-processor quad-core Xeon workstation with 12GB of RAM and using the Pardiso direct solver was approximately 30 minutes. The peak memory usage by Comsol and Matlab 2009b was approximately 4GB. The peak memory requirement was due to a fine mesh used for part of the simulation where the bubble was undergoing its largest deformations. Much of the simulation was performed using 2-3GB of memory. This calculation time does not account for the time spent by the user creating scripts to store solutions, remesh, and pass initial conditions to the next run. The remesh time not

accounted for in this estimate was a relatively short amount of time compared to the overall run time, and would only contribute a couple extra minutes at most. The Pardiso solver did not use all of the available processing cores, even though they were available. The typical CPU load was between 15-50%. The ALE simulation is practical on modern desktop computers with 4GB of memory or more. Other solvers can significantly increase the maximum simulation size by storing data out of memory, such as the Pardiso out-of-core solver.

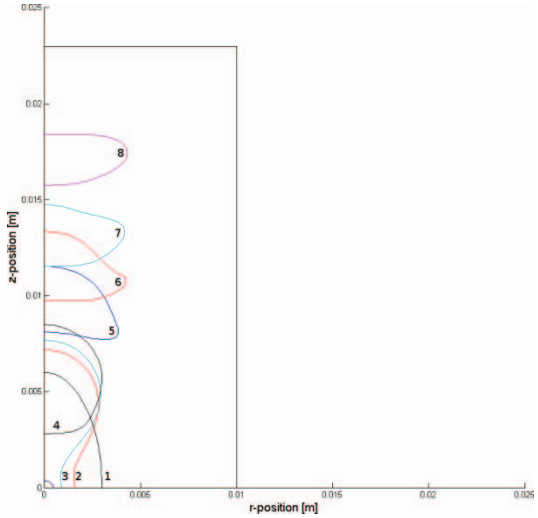

Figure 5. Selected geometry profiles resulting from remeshing during the simulation. The profiles are labeled in chronological order.

Mass conservation in the ALE simulation can be very good. In this simulation relative and absolute tolerances were 0.01 and 1e-3, respectively. Mass conservation can be improved upon in most cases by tightening tolerances, including this simulation. Mesh refinement can help with accuracy too. However, it does increase the simulation time. The mass conservation for the incompressible fluids is shown as a percent change in volume before and after pinch-off in Figures 6-7. Two plots are presented because there is a change in mass at pinch-off because of how the new geometry is created, and not a flaw in the ALE method itself.

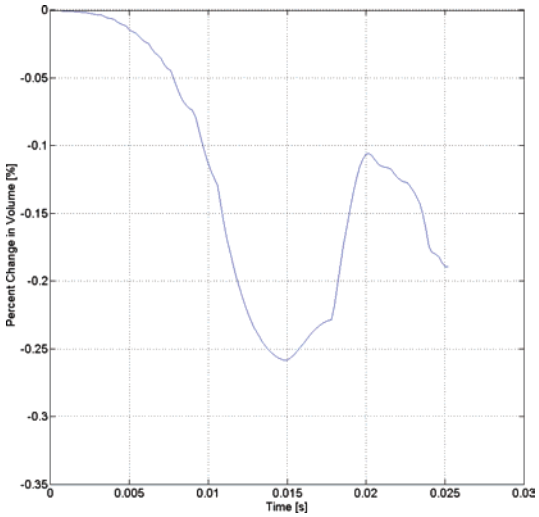

Figure 6. Percent change in volume over the duration of the simulation before pinch-off.

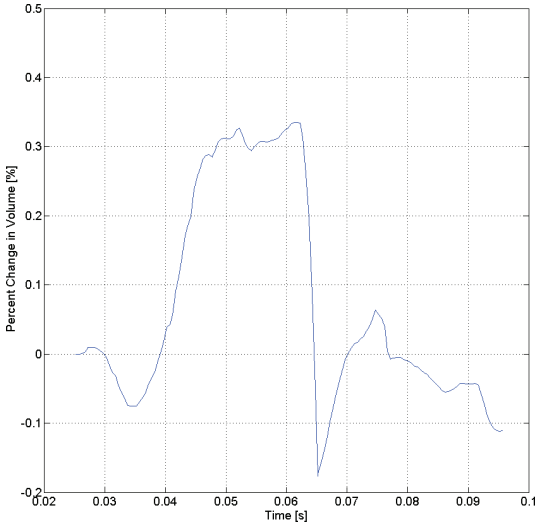

Figure 7. Percent change in volume over the duration of the ALE simulation after pinch-off.

3.2 Level-Set Results in Comparison to ALE

The conservative level-set model was meshed with free triangular elements of maximum volume 0.00015 m^3. The resulting mesh in Figure 8 has 27742 elements with 251007 degrees of freedom.

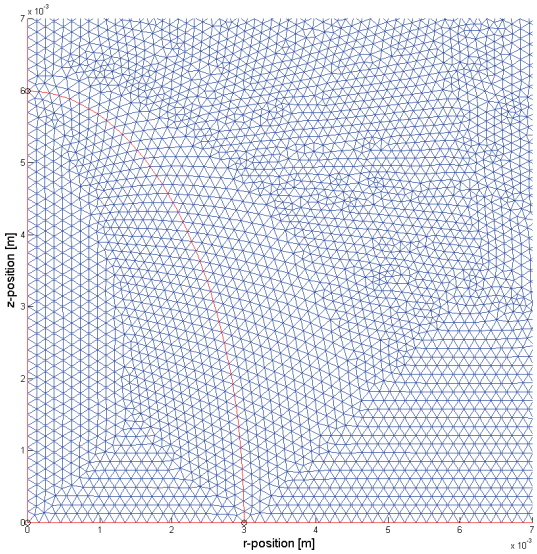

Figure 8. Uniform mesh over entire domain in level-set simulation. Zoomed in to clearly show the mesh density.

The bubble shapes from the conservative level-set simulation are shown in Figure 9. The retraction of the bubble's tail in the level-set method occurs quickly once the filament breaks away. Several small satellite bubbles temporarily formed from the long filament before vanishing or regrouping into larger bubbles. This appears as a jump between the cyan and magenta bubble shapes at the same time steps as in Figure 5. The ALE simulation used a set pinch point and does not allow for formation of satellite bubbles. The formation of satellite bubbles may or may not be an artifact from the evolution of level contours just after the pinch-off point.

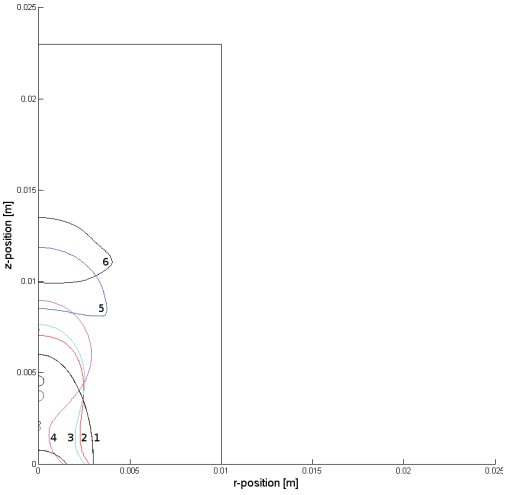

Figure 9. Bubble shapes from the level-set simulation at the same time steps as in Figure 5. The bubble shapes are the contours of phi = 0.5. The level-set simulation failed to find a solution within the default tolerances at approximately t = 0.069 seconds.

3.3 Phase-Field Results in Comparison to ALE

The conservative phase-field model had some trouble getting past pinch-off. The solver would report that a solution within tolerances could not be found. Both mesh refinement and then relaxed relative and absolute tolerances were attempted with no success. This problem may be avoided by adjusting additional model parameters, such as artificial diffusion coefficients, but a solution wasn't found in a timely manner in this situation. A non-conservative phase-field solution is presented instead. The phase-field application mode in Comsol allows for a wetted wall with a specified contact angle, but not a slip condition. The velocity is enforced to be zero at the wall, but some slip still occurs, apparently due to phase tracking. This effect can be seen in Figure 10 as the shapes approach pinch-off more slowly. The boundary condition at the wetted wall makes a significant difference in the time for pinch-off to occur. The slip condition allows the contact patch to shrink more quickly and reduce the neck

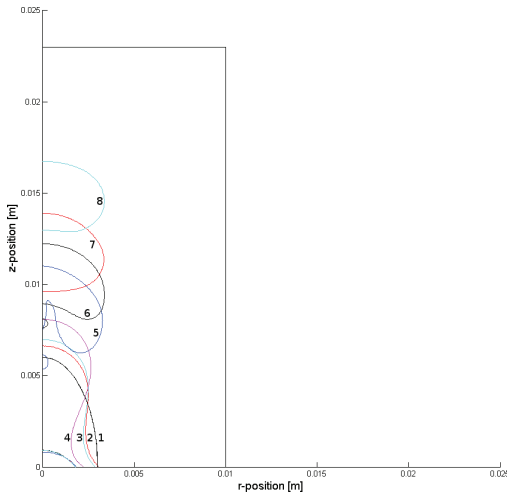

Figure 10. Bubble shapes from the phase-field simulation at the same time steps as in Figure 5. The bubble shapes are the contours of phi = 0.

area sooner. The bubble oscillates less during its ascent, even after a more pronounced inward jet from the tail retracting. As expected with a non-conservative phase-field model, there is a loss of mass over the duration of the simulation. This resulted in a total 8% change in mass for this simulation, occurring gradually over the entire rise of the bubble.

The retraction of the bubble's tail and the inward jet became more pronounced as the mesh was refined in the non-conservative phase-field model. Mass conservation improved with mesh refinement.

3.4 Computational Expense Comparison

The conservative level-set and phase-field models require a relatively dense and uniform mesh to allow the diffuse boundary to approximate a jump condition between fluid phases. This tends to increase the computational expense of the two models. The solution times are provided in Table 2. The value t^* is the ratio of the actual average time to solve for time-steps in the simulation. This makes the comparison between simulation types easier since the simulations ran to different times. All simulations were performed on the same workstation to provide an accurate comparison. The time required for the level-set (LS) and phase-field (PF) models would increase if an iterative solver was used to reduce memory requirements.

Table 2. Solution times for the models.

Model Type	**Solution Time [min]**	**Simulation End Time [s]**	***t*** [min/ms]*
ALE	30	0.096	0.31
LS	700	0.069	10.1
PF Conserv.	280	0.050	5.6
PF, Non-Conserv.	105	0.100	1.05

4. Conclusions

The ALE moving mesh method is capable of handling changes in topology while accurately tracking interfaces and conserving mass. It provides a sharp interface to apply boundary conditions for both the fluid domains and additional application modes. The ALE model appears to have similar bubble shapes as the conservative level-set model. The phase-field model had some differences most likely due to the difference in the wetted-wall boundary no-slip condition. The mass loss may have had a secondary effect on the dynamics of the bubble motion. The times and the locations of the bubble shapes seem to match somewhat between the level-set and ALE models, even though the ALE model included a crude pinch-off procedure.

The fact that the details of the pinch-off process were different for all three models, despite the differences with mesh refinement in the phase-field model, strongly suggests that none of the models currently provide an accurate picture of the pinch-off process. However, the ALE model shows promise because it allows for more control over the pinch-off process than either the level-set or phase-field models. The next step in the development of this pinch-off model is to incorporate an asymptotic computation of the pinch-off process during the time when the length and time scales of the physics become too small to resolve numerically in a reasonable time frame. Once this is accomplished and the results added to the ALE model, a more complete validation of the simulation will be completed.

5. References

1. Gihum Son, Vijay K. Dhir, A Level Set Method for Analysis of Film Boiling on an Immersed Solid Surface, Numerical Heat Transfer, Part B: Fundamentals, Volume 52, 153-177 (2007).
2. Seungwon Shin, Damir Juric, Modeling Three-Dimensional Multiphase Flow Using a Level Contour Reconstruction Method for Front Tracking without Connectivity, Journal of Computational Physics, Volume 180, 427-470 (2002).
3. Herbert Oertel, Ludwig Prandtl, Prandtl's Essentials of Fluid Mechanics, 468-471, Springer-Verlag, New York (2004).
4. C.E. Weatherburn, Differential Geometry of Three Dimensions, 238-242, University Press, Cambridge (1955).